RESEARCH

17(48), 2020

ISSN 2319–7757 EISSN 2319–7765

Indian Journal of Engineering

Optimization of TIG Welding Parameters on the Tensile Strength Performance of Ferritic Stainless Steel Welds Using Response Surface Methodology

Musa AA✉, Dauda ET, Bello KA, Adams SM

Department of Metallurgical and Materials Engineering, Ahmadu Bello University, PMB 1045, Zaria, Nigeria

✉**Corresponding author:**
Email address: abdulrahman@abu.edu.ng; Tel: 08039162744.

Article History
Received: 10 October 2020
Accepted: 22 November 2020
Published: December 2020

Citation
Musa AA, Dauda ET, Bello KA, Adams SM. Optimization of TIG Welding Parameters on the Tensile Strength Performance of Ferritic Stainless Steel Welds Using Response Surface Methodology. *Indian Journal of Engineering*, 2020, 17(48), 591-604

ABSTRACT

In this study, influence of tungsten inert gas (TIG) welding process parameters on the tensile strength of AISI430 ferritic stainless steel welds was investigated. Response surface methodology, based on the central composite design (CCD) was employed to plan and design the experiment. The three input factors considered in this study Include; the welding current (I), welding speed (S) and gas flow rate (GFR). It was observed that all the three input factors directly influence the tensile strength of the weldment. The welding current has the most influential effects on the tensile strength with about 34% contribution, followed by the speed with 15% and the least contribution was the gas flow rate. Empirical models were generated from the obtained responses to predict the weld quality. An optimized tensile strength of 431.014MPa was predicted at the welding current of 22A, the welding speed of 5mm/sec and the argon flow rate of 10L/min. The results were validated by performing a Confirmatory experiment in order to check the

practicability of the developed models. Hence the test results were in good agreement with the predicted values with average percentage errors of 1.63% which is within the acceptable value for adequate model as per Design-Expert.

Keywords: Tensile strength, Grain growth, Heat input, Stainless steel, TIG welding techniques

1. INTRODUCTION

Gas metal arc welding also known as tungsten inert gas welding (TIG) is one of the commonly used arc welding technique for joining different materials used in critical industries such as pipelines and oil and gas industries (Vijayan, 2018). During fabrication of stainless steel components or equipment, manufacturers usually employ tungsten inert gas welding process as the principal joining method. This is because TIG welding is specifically designed for welding materials with minimum heat energy input. Tungsten Inert Gas (TIG) welding is an arc welding process that produces coalescence of metals by heating them with an arc established between a non-consumable tungsten electrode and the work piece with or without filler metal depending on the thickness of the workpiece (Lokesh *et al.*, 2015). TIG welding process produces high quality welds joint and is suitable for joining thin and medium thickness material like aluminum and its alloys, titanium and its alloy, low alloy steels and stainless and steels (Cibi *et al.*, 2017).

Stainless steels are important class of materials developed for applications, especially in corrosive environments; these steels possess good corrosion resistant due to the formation of thin protective oxide layer on the surface (Ravinder and Jarial, 2015). They also exhibit better strength at high temperature, toughness at cryogenic temperature, and fabrication characteristics which makes their selection for industrial applications very popular. They are used for the demanding requirements of chemical processing to the delicate handling of food and pharmaceuticals. They are preferred over many other materials due to their excellent performance even in the most aggressive environments, and they are fabricated by methods common to most manufacturers (Amuda *et al.*, 2012).

They are weldable materials, producing a welded joint with optimum strength, fabrication economy as well as corrosion resistance. However, designers should note that any metal, including stainless steels, may undergo certain structural changes during welding. It is therefore, necessary to exercise a reasonable degree of care during welding to minimize and prevent any deleterious effects that may occur by selecting the proper welding process and controlling the welding conditions.

One major problem that limits the industrial application of stainless steel is the loss of properties such as strength, ductility and impact toughness in the weld section due to the intense welding heat that induces grain coarsening to the weld joint (Amuda and Mridha, 2010).

Hence, the present study investigates the influence of TIG process parameters on tensile strength and percentage elongation of AISI430 ferritic stainless steel welds and using Design-Expert based on response surface methodology (RSM) approach.

2. EXPERIMENTAL PROCEDURE

2.1 Materials and sample preparation

The materials used in this study is ferritic stainless steel (AISI430grade) of 1.5mm thickness. It was purchased from CencoSains Company, Malaysia. The chemical composition of the stainless steel is given in Table 1.

Table 1: chemical composition of AISI 430 ferritic stainless steel

Element	C	Si	Mn	P	S	Cr	Ni	Mo	Fe
% composition	0.12	0.75	1.00	0.040	0.030	16-18	-	-	balance

2.2 Central Composite Design

Central Composite Design (CCD) is a type of response surface methodology which involves sequential steps of experimentation with 2^n factorial points augmented by additional central and 2n star or axial points. Factorial points provide estimation linear and interaction terms, while the star points and center run gave the presence of curvature and error respectively (Diler and Ipek, 2012). Because of the rotatability of CCD, it is capable of providing an equal precision of estimation in all direction. Considering a factorial point of each factor ±1 unit away from the center of the design region, the axial (star) points will be given as ±α such that | α | > 1. The value of α depends on the number of the input factors and other properties. For a rotatable design and full factorial experiment, α can be estimated using equation 1.

$\alpha = (2^n)^{1/4}1$

Where n is the number of input factors

Central composite design (CCD) has been selected in this study to plan and design the experiment. The three factors were varied over five levels as -α, -1,0, +1, +α which represent the factorial points, axial/star point and additional center runs. The factorial levels chosen for the current are 15A and 25A, while the values of 3mm/s and 5mm/s as well as 6L/min and 10L/min were selected for the speed and the argon flow rate respectively. The input factors and their levels are presented in Table 2.

Table 2: Factors and levels for the CCD experimental design plan

Factors	Symbol		Levels				
	Equation	Design	-2	-1	0	1	2
Welding current (A)	X_1	*A*	10	15	20	25	30
Welding speed (mm/s)	X_2	*B*	2	3	4	5	6
Argon flow rate (L/min)	X_3	*C*	4	6	8	10	12

2.3 TIG torch Welding Technique

The experiments were performed using Clarke 101 Inverter TIG welding machine shown in Fig 1. The TIG welding machine used non-consumable tungsten electrode which contain 2% thorium and 2.5mm tip diameter. Straight polarity (DCEN) was employed for the autogenous TIG welding of ferritic stainless steel. Pure argon gas was used as the shielding gas at a variable flow rates using a flow meter gauge.

Fig 1: TIG welding machine setup

The sample (AISI 430 FSS) of thickness 1.5mm was sectioned into a dimension of 120mm x 90mm using cutting machine. It was then cut into two equal parts along the width and then butt weld using TIG welding method. Tensile test specimens were cut from each of the welded plates for the determination of the tensile properties. Experiment with the 20 trials was conducted and the results were recorded. A minimum of three samples were considered for each trial and the average values recorded for respective responses.

2.4 Tensile Test

Tensile test also known as tension test is one of the most fundamental and common types of mechanical testing. In this research study, three tensile specimens were machined from each of the welded samples as shown in figure 3.2 and prepared to conform to the standard of the tensile machine used for the tensile testing.

Figure 2 Tensile test specimens

The samples were subjected to tensile tests in accordance with ASTM E8 standard method. Each of the samples was mounted by its both ends, gripped into the Hounsfield Tensometer, Type W with a capacity of 20kN and elongated at a constant rate by a tensile force. The applied load/force and the elongation were measured simultaneously by cell load and extensometer respectively. The test was carried out at the Department of Mechanical Engineering, Ahmadu Bello University, Zaria.

2.5 Experimental Design Matrix and Measured Response

Circumscribed type of central composite (CCC) design with three factors at five levels was chosen for the experimental design, and this represent the case of second-order modeling for the responses.

The total number of experimental runs is estimated using $2^k + 2k + 6$, with 8 factorial points (2^k), 6-star points (2k) and 6 central runs to make up a total of 20 experimental runs, i.e. $2^3 + 2(3) + 6 = 8+6+6 = 20$ runs.

Where k is the number of input factors, and the central run is chosen as six (6) for convenience and accuracy especially when the input factors is more than two.

To conclude, the factors with their levels and the responses were entered in the CCC design of the Design-Expert version 10 to generate the overall matrix for the analysis as shown in Table 3.

Table 3: design matrix and responses for process parameters of TIG welding process

Run	Factor			Response
	A: Welding Current (A)	**B: Welding Speed (mm/s)**	**C: Argon Flow Rate (L/min)**	**Tensile Strength (MPa)**
1	15	3	10	253.3
2	20	4	8	360
3	20	4	8	364.4
4	15	5	10	401.1
5	15	3	6	293.5
6	25	3	10	263.6
7	20	4	8	366.7
8	20	6	8	400
9	10	4	8	200
10	25	3	6	384.4
11	20	4	12	355.6
12	20	2	8	340
13	20	4	8	370
14	30	4	8	364
15	15	5	6	250
16	25	5	6	390.5

17	20	4	8	342.2
18	25	5	10	431.1
19	20	4	8	344
20	20	4	4	348

3. RESULTS AND DISCUSSION

3.1 Fit-summary Analysis of the Model

The fit summary statistics analyses the relationship between the independent variable and the response by the regression analysis in order to fit all the models to the selected responses. The highest order polynomial with significant term for the tensile strength has F-value of 12.87 at P ≤ 0.0009 as presented in Table 4 and the highest order of polynomial suggested by the model is the quadratic as indicated in the Table.

Table 4 Fit Summary statistics for Tensile strength

Source	Sum of Squares	df	Mean Square	F Value	P-value Prob > F	
Mean vs Total	2.327E+006	1	2.327E+006			
Linear vs Mean	32504.46	3	10834.82	5.05	0.0119	
2FI vs Linear	20714.87	3	6904.96	6.58	0.0061	
Quadratic	**10832.00**	**3**	**3610.67**	**12.87**	**0.0009**	**Suggested**
Cubic vs Quadratic	1883.15	4	470.79	3.06	0.1072	Aliased
Residual	923.01	6	153.83			
Total	2.394E+006	20	1.197E+005			

3.2 ANOVA test results for the tensile strength

The analysis of variance for the tensile strength with all the model terms is presented in Table 5. It can be observed from the Table that the model is significant having a p-value less than 0.05. The analysis of variance was carried out at 5% significance level or 95% confidence level. Also, the lack of fit for the model is greater than 0.05 which means, it is not significant which is desirable.The "Lack of Fit F-value" of 0.1476 implies the Lack of Fit is not significant relative to the pure error since it value is greater than 0.05. There is a 14.76% chance that a "Lack of Fit F-value" this large could occur due to noise. Non-significant lack of fit is good, we want the model to fit. Equation1 and 2 represent the model equation to predict the ultimate tensile strength (UTS) based on the process parameter variable with significant model terms (A, B, AC, BC and A^2) as shown in the ANOVA Table. The model equations were developed from the improved analysis of variance by removing all the model with insignificant terms. Equation 1 identifies the relative impact of each parameter on the ultimate tensile strength based on the coefficient of each of the variable. From the equation, it can be observed that the most influential parameter on the tensile strength in the order of important is the welding current, welding speed and the argon flow rate.

While equation 2 can be used to make predictions about the response for given levels of each factor. Here, the levels should be specified in the original units for each factor. However, the equation cannot be used to determine the relative impact of each factor because the coefficients are scaled to accommodate the units of each factor and the intercept is not at the center of the design space.

Table 5 Analysis of variance (ANOVA Table) for the tensile strength

Source	*Sum of Squares*	*df*	*Mean Square*	*F Value*	*P-value Prob > F*	
Model	*63119.19*	*6*	*10519.87*	*36.58*	*< 0.0001*	***significant***
A-Current	*22477.51*	*1*	*22477.51*	*78.17*	*< 0.0001*	
B-Speed	*9895.28*	*1*	*9895.28*	*34.41*	*< 0.0001*	
C-Argon flow rate	*131.68*	*1*	*131.68*	*0.46*	*0.5105*	
AC	*4564.90*	*1*	*4564.90*	*15.87*	*0.0016*	
BC	*15549.66*	*1*	*15549.66*	*54.07*	*< 0.0001*	
A^2	*10500.17*	*1*	*10500.17*	*36.51*	*< 0.0001*	

Residual	*3738.30*	*13*	*287.56*			
Lack of Fit	*3028.09*	*8*	*378.51*	*2.66*	*0.1476*	***not significant***
Pure Error	*710.21*	*5*	*142.04*			
Cor Total	*66857.49*	*19*				

Model Equation in terms of coded factors

$UTS = +356.84 + 37.48A + 24.87B + 2.87C - 23.89AC + 44.09BC - 19.65A^2$(1)

Model Equation in terms of actual factors

$UTS = +104.79853 + 58.04272 x current -151.48125 x speed – 38.96563 x argon\ flow\ rate – 2.38875 x current\ x argon\ flow\ rate + 22.04375\ x\ speed x argon\ flow\ rate – 0.78591 x current^2$(2)

The perturbation plot shown in Figure 4 represents the effects of each of the process parameters on the tensile strength. From the plot, it can be seen that current has the most influence on the tensile property which increases gradually from the reference point to a maximum and decreases at higher current which confirm that the current has a quadratic effect on the response as suggested in the fit-summary (Table 4). The argon flow rate is almost linear which indicates that it has little significant on the tensile strength.

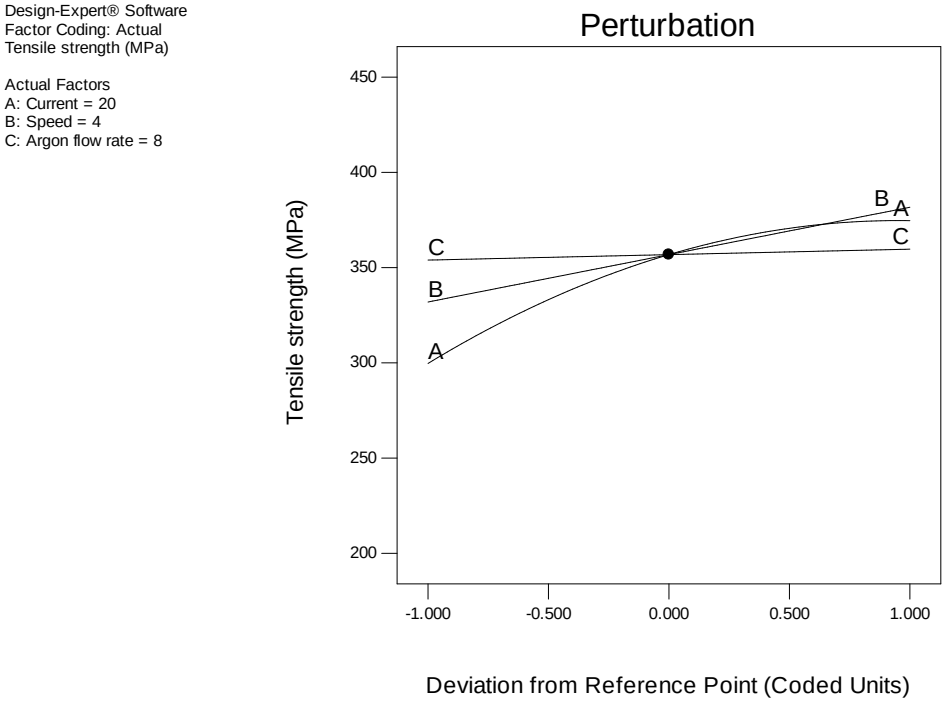

Figure 4 Perturbation plot for Tensile Strength

3.3 Model Adequacy Assessment

The model adequacy is analytically verified by assessing the following model tool which include; the normal plot of residual (Fig 5), residual plot versus predicted value (Fig 6), residual versus run (Fig 7) and the Box-cox plot for power transformation shown in fig 8. The normal probability plot of the residuals for the tensile strength shown in Fig5 reveals that the residuals (errors) are falling on the straight line, which means the errors are distributed normally (Abhulimen and Achebo, 2014). This clearly indicates an excellent adequacy of the regression model based on the RSM design expert. Fig 6 shows the plot of residual versus predicted values for the tensile strength and it can be seen that the data did not follow any definite pattern but within the accepted limit, hence, the data is considered to be adequate to predict the tensile strength.

Fig 7 presents the plot of residual against the run order which also satisfy the adequacy requirement of the model by showing a randomly scattered values without any relationship towards either of the two ends, indicating the adequacy of the model. The last model tool used to assess the adequacy of the developed model is the Box-Cox transformation shown in fig 8.

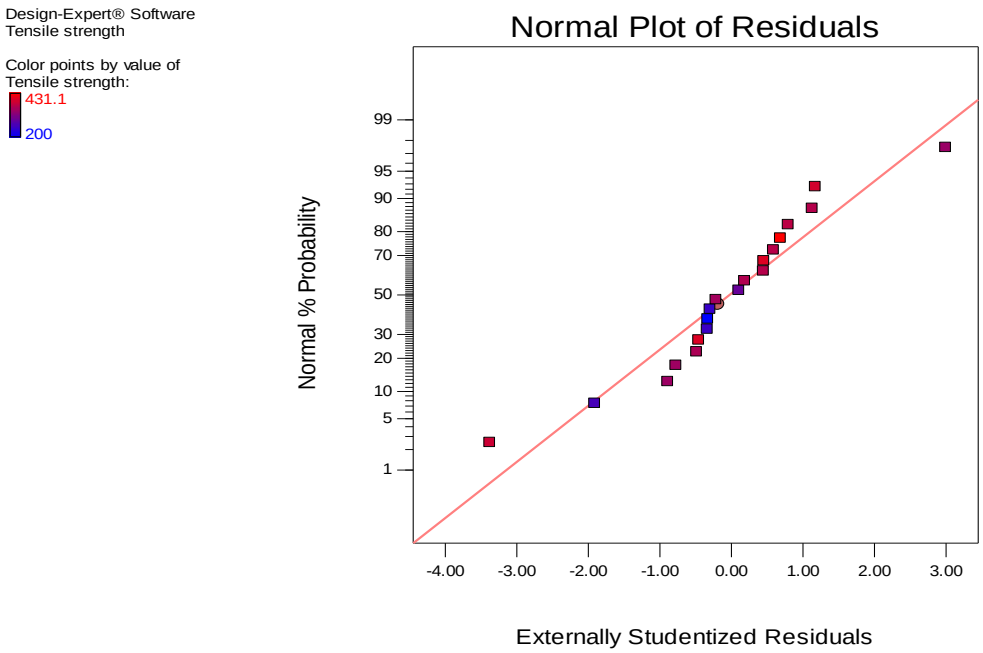

Figure 5. Normal probability plot of residuals for tensile strength

The Box-Cox transform the non-normal dependent variable into a normal shape. The curve preforms data analysis on the response factor by providing a confidence interval on the transformation parameter (Lambda) based on the result. The analysis is normally performed to show whether or not a transformation is needed. Transformations are normally performed when there is need to normalize the dependent variable or stabilize the variance in order to improve the model (Adebisi, 2016), This usually occur when the confidence level is not unity. Therefore, since it is observed from fig 8 that the value of λ (confidence level) is unity, no transformation is recommended to the model. Hence, it can be concluded that the normality and residual displayed from the Box-Cox plot are adequate to predict the tensile strength

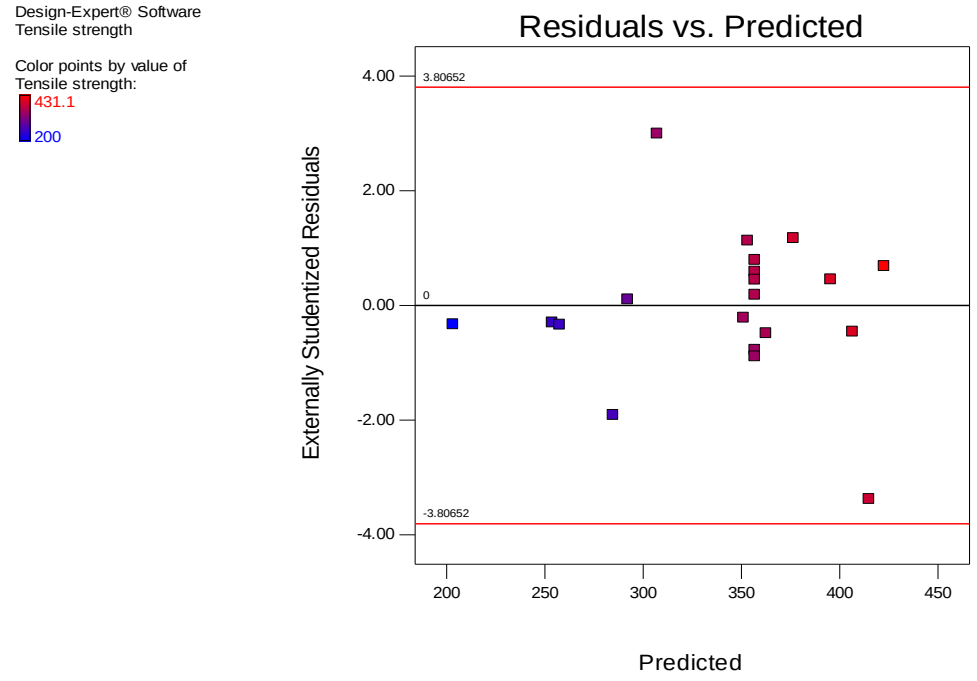

Figure 6. Plot of residual against predicted values for Tensile strength

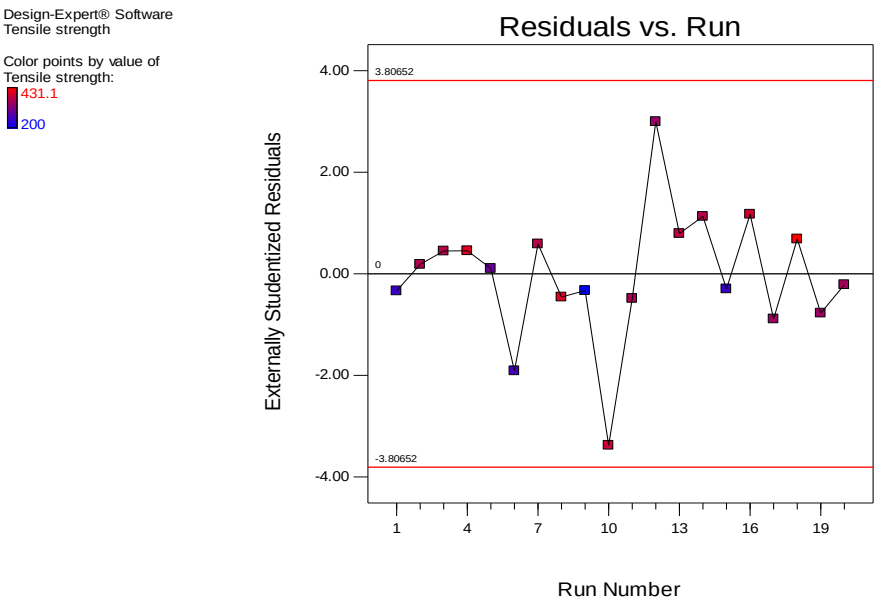

Figure 7. Plot of residual versus experimental run order for Tensile strength

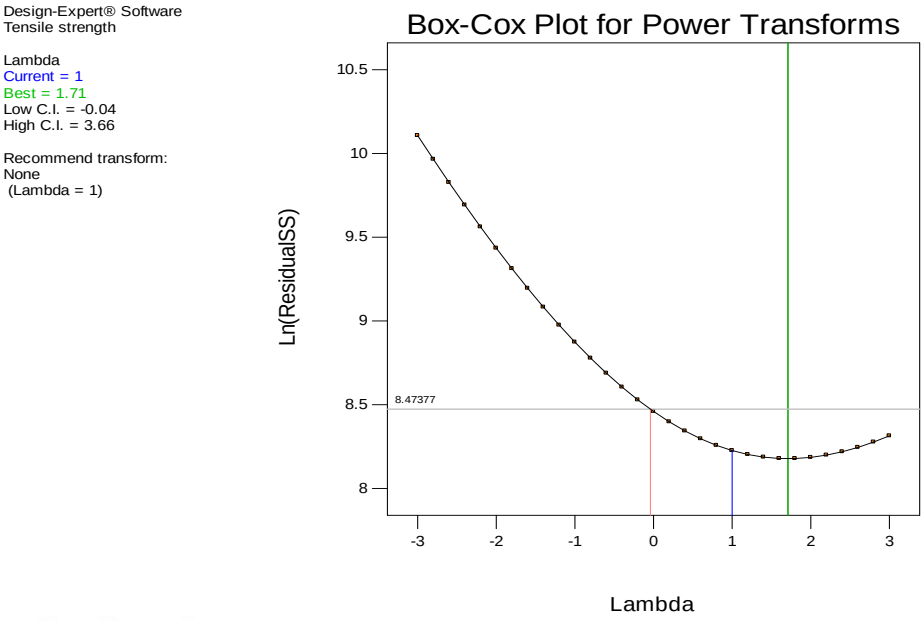

Figure 8. Box-Cox plot for Tensile strength

3.4 Model Graphs and Discussions

The model graphs for the tensile strength response which include both the 3-D surface graphs and contour maps are presented in Fig 9 - 11 below. In the surface plots the input variables are shown in x and y axes while the response is presented on the z axis, which ultimately reveal the optimal level. The graph shown in Fig 9 (a) and (b) represents the effect of the interaction between two factors (current and argon flow rate) on the response (tensile strength). It can be observed from the plots that the tensile strength is minimum at a current of 10A and argon flow rate of 4L/min. It increases gradually with increase in the current with very little rise in the flow rate and peak at about 26A. As the flow rate is further increased to 12L/min, the tensile strength reduces even though there are no significant changes in the current. This clearly showed that the current and the gas flow rate has positive effect on the tensile strength of the weldment. However, the effect of the gas flow rate is minimal compared with that of the current. The trend displayed by the tensile strength in Fig 10 is different from Fig 9, as the tensile strength increases with increase in both current and the welding speed. Maximum value of tensile strength was achieved at a current of 25A and speed of 5mm/s. As the current increases further to 30A and at a speed of about 3mm/s, there is a decrease in the tensile strength. This trend of result is very similar to the study conducted by Subhas, *et al.* (2019). The decrease in the tensile strength at higher current and lower speed may be due to the

too much heat energy input into the welded joint which may induces coarse grains in the weld and heat affected zone, thereby reducing the properties of the weldment (Subhas, *et al*. (2018). Fig 11 shows the interactions between the speed and the gas flow rate on the tensile strength, and it can be observed from the graphs that the tensile strength is minimal at a flow rate of 12L/min and a speed of 2mm/s. the tensile strength increases gradually as the gas flow rate decrease while the speed remains constant at 2mm/s. Similarly, the tensile strength also peaks at higher speed of 6mm/s and at a flow rate of 12L/min. These results confirm the significant interaction between the speed and the flow rate having a value less than 0.05 as shown in the ANOVA Table.

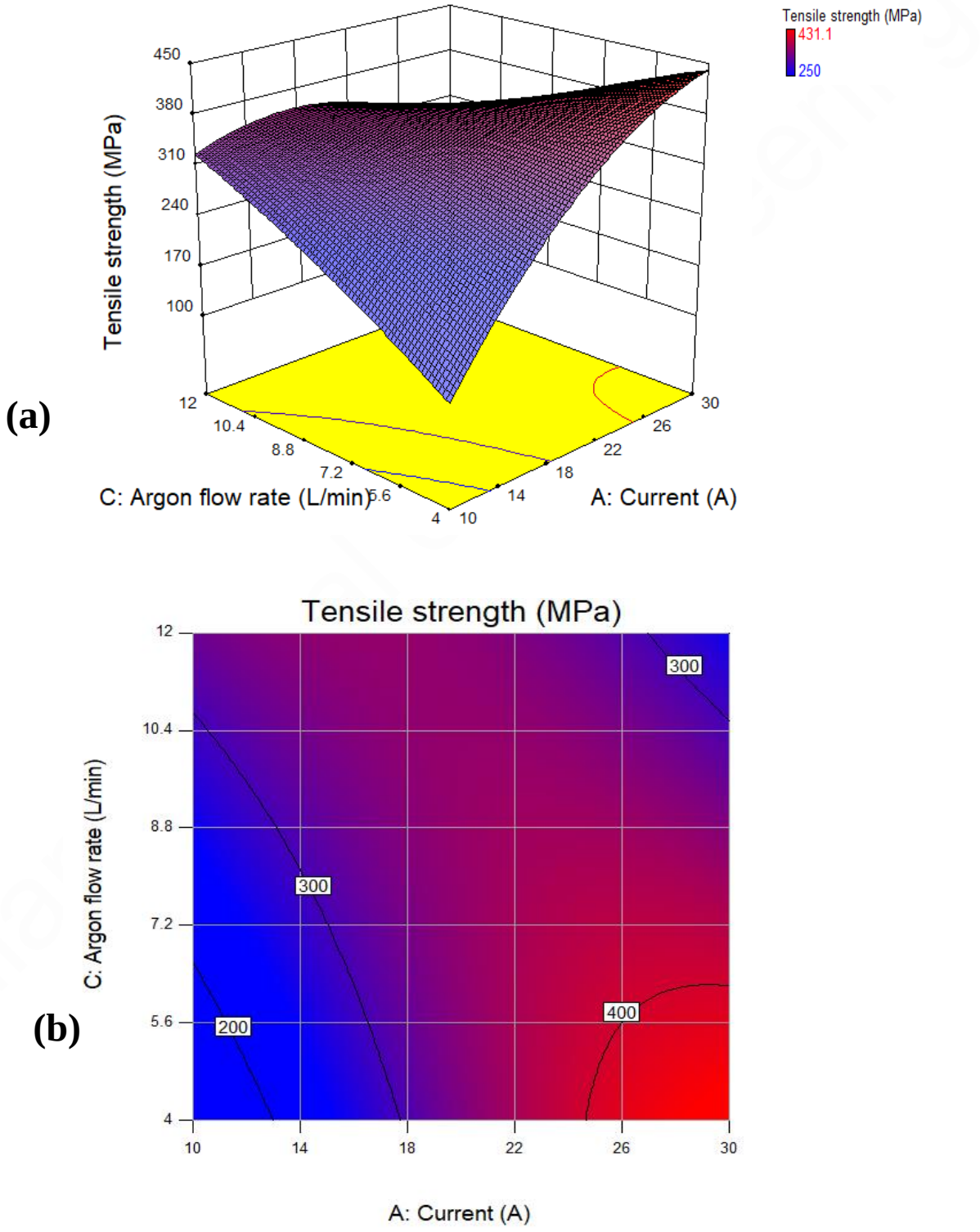

Figure 9: 3-D surface and contour plot showing the variation of Tensile strength with welding current and gas flow rate (a) 3-D surface plot (b) Contour plot

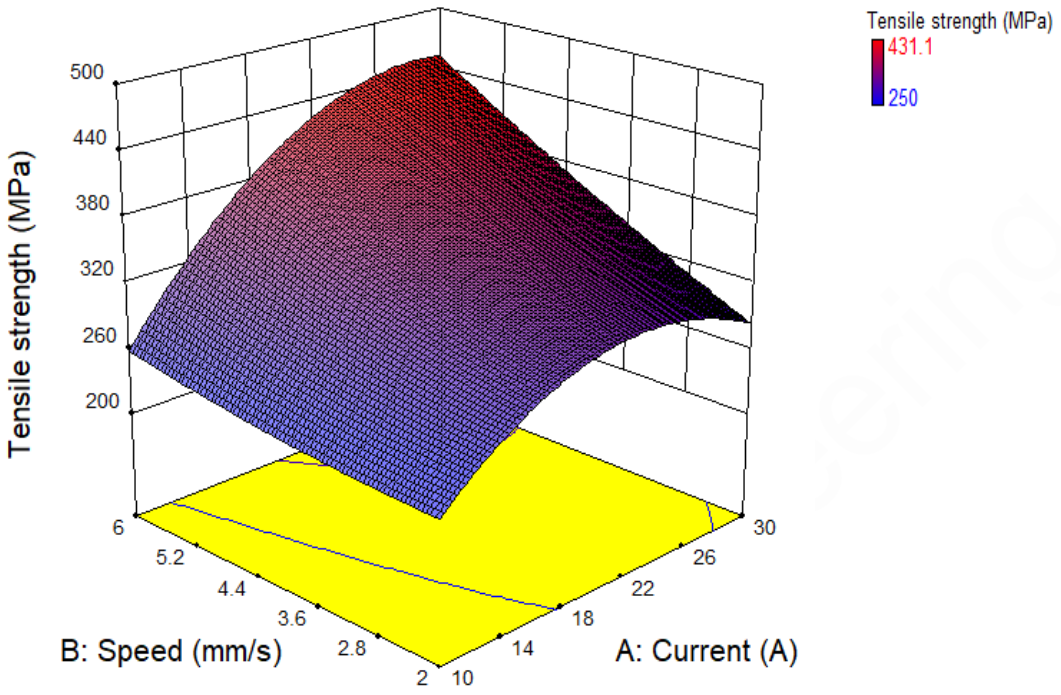

(a)

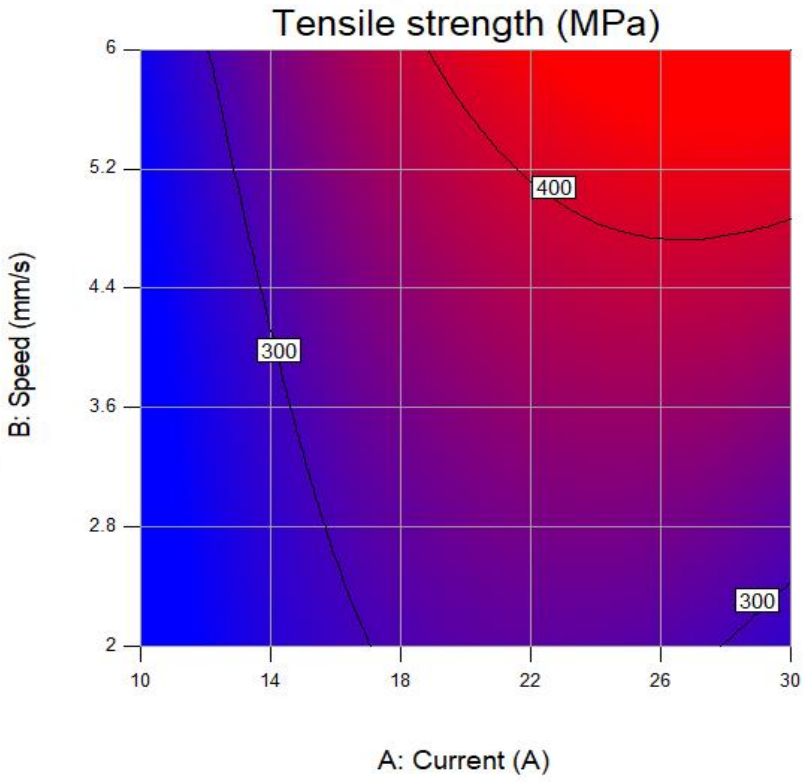

(b)

Figure 10: 3-D surface and contour plot showing the variation of Tensile strength with welding current and welding speed (a) 3-D surface plot (b) Contour plot.

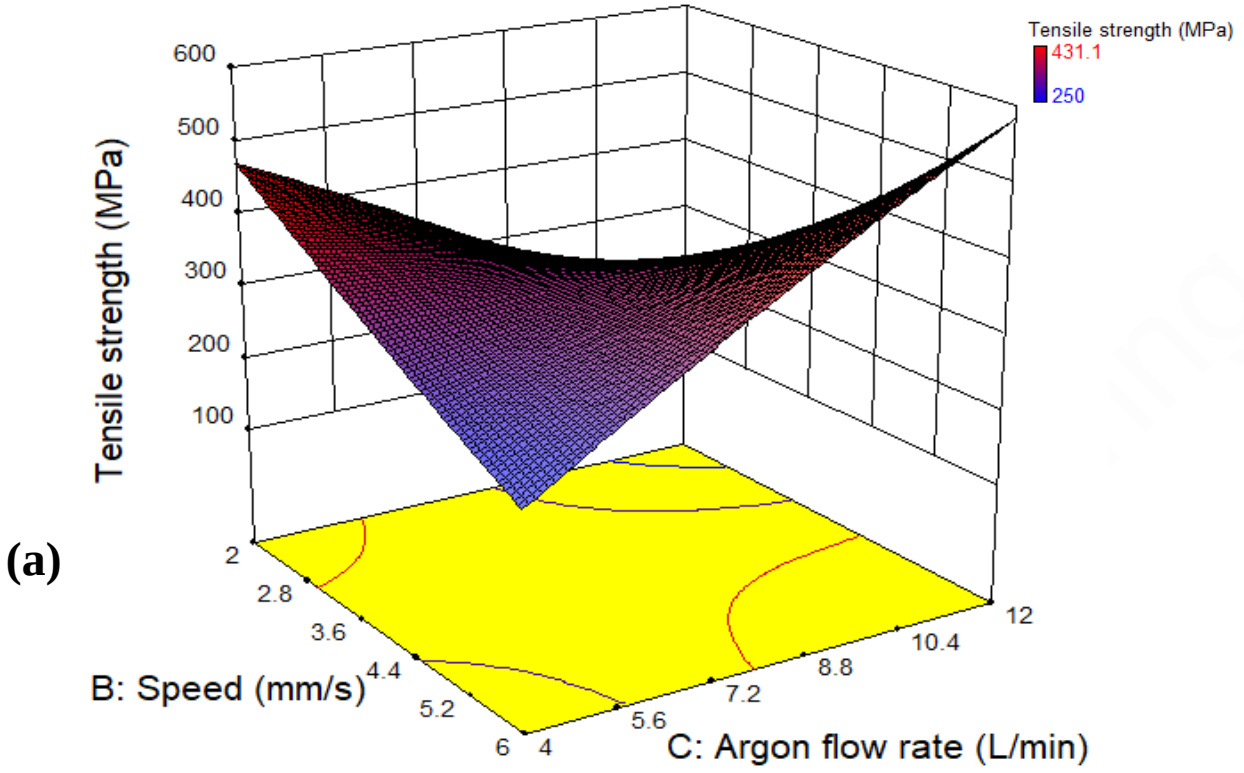

(a)

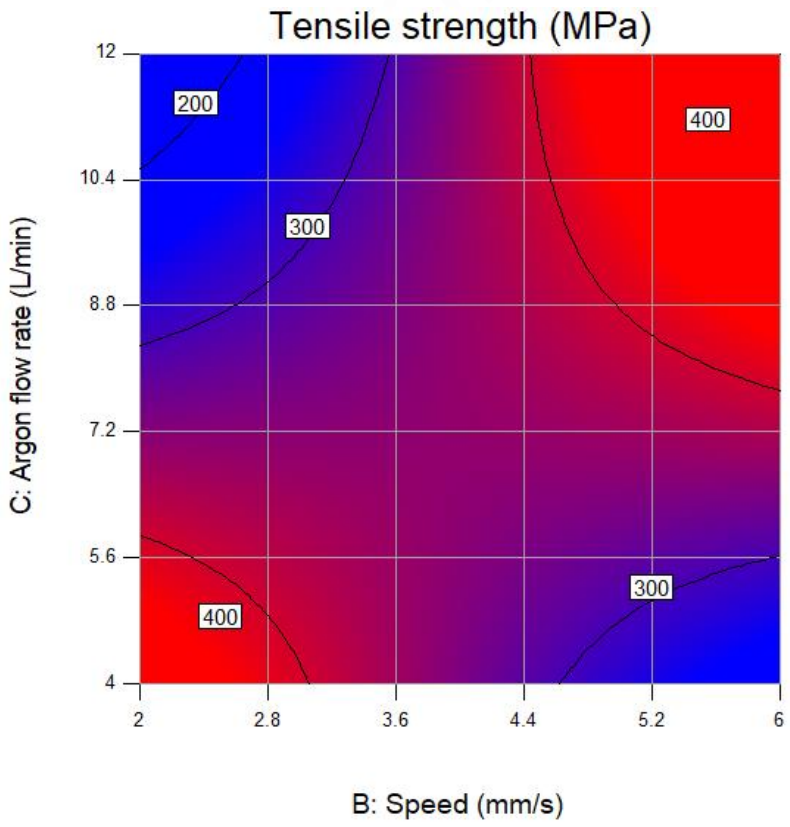

(b)

Figure 11: 3-D surface and contour plot showing the variation of Tensile strength with welding speed and the argon flow rate (a) 3-D surface plot (b) Contour plot.

3.5 Confirmation test Results

In order to validate test results of optimization generated from the developed model, confirmatory tests were also performed using the predicted process parameters and compared with the predicted responses. Two confirmatory tests were performed as presented in Table 6 and the average percentage error was calculated. It can be observed from the Table that the predicted and observed results are in a good agreement with average percentage error of 1.63 which is within the satisfactory range of percentage error (Vidyarthy et al. 2017).

Table 6 Confirmation test results

Test No.	Process Parameter			Tensile Strength (MPa)		
	Current (A)	Speed (mm/s)	Argon flowrate (L/min)	Predicted	observed	% Error
1	21.737	5	10	431.014	425.705	1.23
2	22.440	5	10	430.618	421.924	2.02

3.6 Characteristics of optimized TIG ferritic stainless steel weld

Table 7 presents the tensile strength of both the base metal and the welded sample with optimized process parameters.Based on this result, it can be seen that the FSS weld has close tensile strength with the base metal which is the aim of the current study.

Table 7 Mechanical properties of base metal and welded metal with optimized parameters

Material	Tensile strength (MPa)	% Elongation
Base metal	446.7	38.8
Welded sample with optimized parameters	431.014	28.3

3.6.1 Weld Topography

The topographies of the weld tracks produced under different process parameter conditions are shown in Figure 12 (a-c). Since welding current appears to be the most prominent factor controlling the weld quality, the topographies of the weld metal assessed were selected based on the current variations which corresponds to run no. 9, run no.14for lower and higher current respectively, as well as optimized condition. The surface of the welds wascaptured with a high resolution 14Mp Panasonic digital camera. It can be observed that the topography of the optimized weld (Figure 12(c)) is smoother, continuous and defect free compared to welds at the two extreme currents. Weld at very low current in Figure12(a) showed the existence of porosities along the weld track, while in Figure 12(b), there is evidence of high heat energy into the weld joint withpoor weld surface quality.

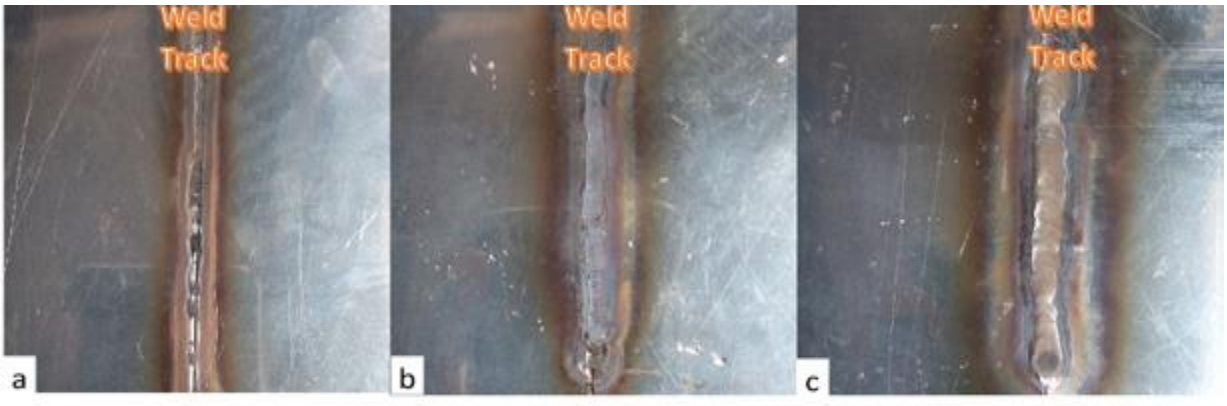

Figure 12 Topographies of the welds under different grain welding conditions: (a)10A (b) 30A(c) optimized condition

3.6.2 Analysis of the Tensile strength

Figure 13 shows the influence of welding current on the tensile strength of the optimized TIG ferritic stainless steel weld by keeping the other variables constant. It is observed that the effect of current and speed exhibit a parabolic behaviour on the tensile strength

with its maximum value at 22A and 5mm/s as shown in Figure 13 and 14 respectively. It can be seen that the strength was maximum at the optimum values of the welding current and speed and decrease below and above the optimum value.

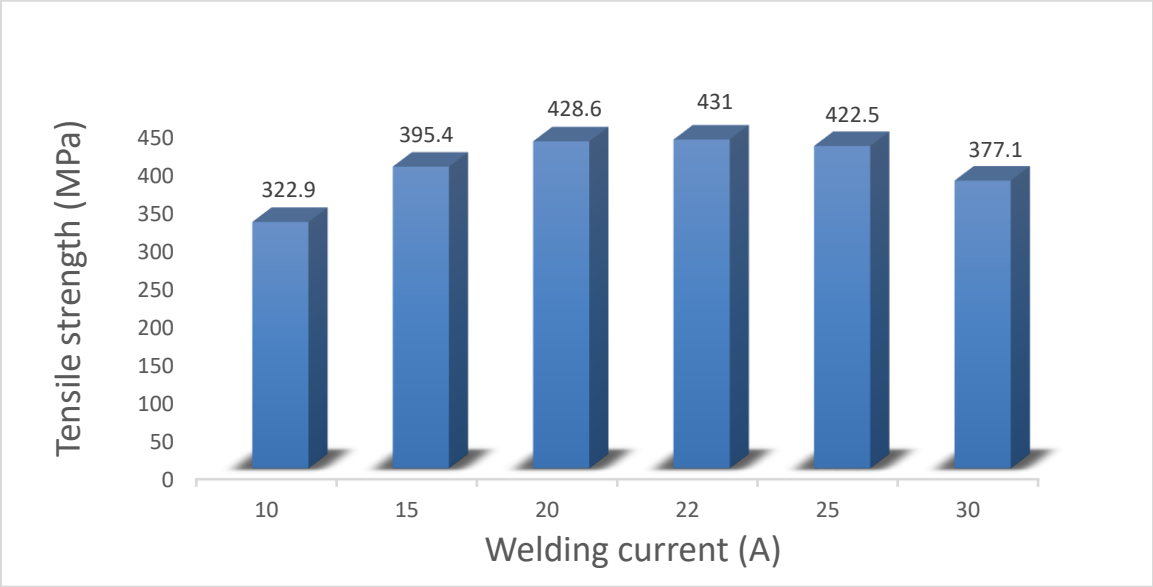

Figure 13 Influence of welding current on the tensile strength for the optimized welds

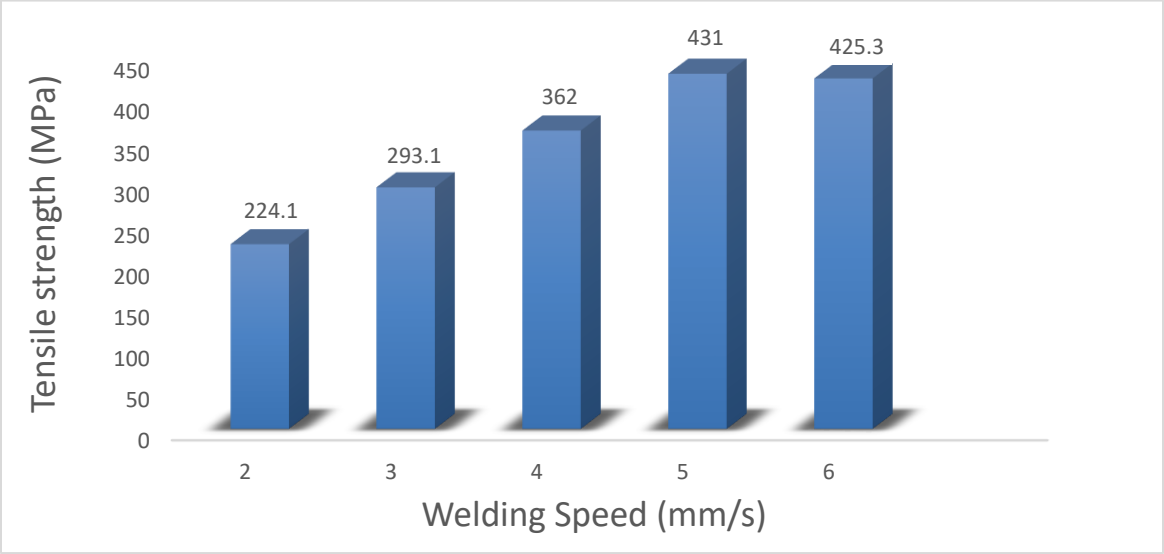

Figure 14 Influence of welding speed on the tensile strength for the optimized welds

4. CONCLUSIONS

In the present study, the influences of TIG process parameters on the tensile strength of ferritic stainless steel (AISI430 grade) welds was investigated and the following conclusions were drawn;

1. The topography of the optimized weld is continuous, smooth and defect free compared to welds at the two extreme heat inputs. Hence, the produced TIG ferritic stainless steel welds with improved weld quality was successfully achieved through the optimization process.
2. The welding current was found to be the most influential factor on the tensile strength with 34% contribution, followed by welding speed of 15% and 2.54% for the argon flow rate.
3. The optimized tensile strength of 431.01MPa was achieved at a welding current of 22A, welding speed of 5mm/s and the argon flow rate of 10L/min.

4. The confirmation experiment was successfully performed to validate the modeling and optimization of the process. The average percentage error of 1.63%was estimated between the actual and the predicted value, which is within the accepted range as per RSM design method.

Conflict of interests

There is no conflict of interest among the authors.

Funding

There is no direct funding for this project.

Peer-review

External peer-review was done through double-blind method.

Data and materials availability

All data associated with this study are present in the paper.

REFERENCE

1. Abhulimen, I.U. and Achebo, J.I. (2014). Prediction of Weld Quality of A-Tungsten Inert Gas Welded Mild Steel Pipe Joint Using Response Surface Methodology (RSM). *Int. Journal of Engineering Research and Applications,* 4(8), pp.31-40
2. Adebisis A.A. (2016). Optimization of stir casting process parameters of Aluminium Silicon Carbide Particulate composites. PhD thesis, pp. 145.
3. Amuda, M.O.H, Mridha S. (2010). Grain refinement in ferritic stainless steel welds: the journey so far. *Advanced Materials Research Vols. 83-86 (2010) pp. 1165-1172.*
4. Amuda, M.O.H., and Mridha, S. (2012). Comparative evaluation of grain refinement in AISI 430 FSS by elemental powder addition and cryogenic cooling. Materials and Design, 35, pp. 609-618
5. Cibi, A. J, and Thilagham, K T (2017). High Frequency Gas Tungsten Arc Welding Process for Dressing of Weldment. *International Journal of Advanced Engineering Research and Science (IJAERS)*, 4(3), pp. 229-235.
6. Diler, E.A. and Ipek, R. (2012). An experimental and statistical study of interaction effects of matrix particle size, reinforcement particle size and volume fraction on the flexural strength of Al-SCp composite by P/M using central composite design. *Materials Science and Engineering.* 548, pp. 43-55
7. Lokesh, K.G., Karthikeyan, P., Narasimma, R.C., Prasanna, B. and George, O. (2015) Microstructure and Mechanical Properties of ASS (304)-FSS (430) Dissimilar Joints in IN SMAW and GTAW Process. *International Journal of Engineering Sciences and Research Technology*, 6, pp. 367-378.
8. Ravinder, S. K. Jarial. (2015). Parametric Optimization of TIG Welding on Stainless Steel (202) and Mild Steel by using Taguchi Method. *International Journal of Enhanced Research in Science Technology & Engineering*, 4 (6), pp. 484-494.
9. Subhas, C. M., Pradip, K.P. and Asish, B. (2019). Design Optimization of TIG Welding Process for AISI 316L Stainless Steel. *International Journal of Recent Technology and Engineering (IJRTE)*, 8(2), pp. 5348-5354
10. Subhas, C. M., Pradip, K.P., Asish, B. and Rudrapati, R. (2018). Determination of tungsten inert gas welding input parameters to attain maximum tensile strength of 316l austenitic stainless steel. *Journal of Mechanical Engineering*, 68(3), pp. 231 – 248.
11. Vidyarthy, R. S., Dwivedi, D. K and Vasudevan, M. (2017). Optimization of A-TIG Process Parameters Using Response Surface. *Materials and Manufacturing Processes*. pp. 1-31.
12. Vijayan, D., Seshagiri, V.R. (2018). Process Parameter Optimization in TIG Welding of AISI 4340 Low Alloy Steel Welds by Genetic Algorithm. IOP Conf. Series: Materials Science and Engineering (390) 012066 doi:10.1088/1757-899X/390/1/012066.